Fibers and Polymers 2011, Vol.12, No.4, 444-450 DOI 10.1007/s12221-011-0444-2

Preparation of New Polymer Nanocomposites Based on Poly(lactic acid)/Fatty Nitrogen Compounds Modified Clay by a Solution Casting Process

Emad A. Jaffar Al-Mulla

Department of Chemistry, College of Science, University of Kufa, AnNajaf, Iraq
(Received March 29, 2010; Revised January 1, 2011; Accepted January 18, 2011)

Abstract: In this study, different organoclays (OMMTs) were prepared using various fatty nitrogen compounds (FNCs) and natural clay, sodium montmorillonite (MMT). The clay modification was carried out by stirring the clay particles in an aqueous solution of fatty amides (FA), fatty hydroxamic acids (FHA), and carbonyl difatty amides (CDFA). These OMMTs were then used for nanocomposites production to improve the property balance of poly(lactic acid) (PLA) by solution casting process. All sets of OMMTs and nanocomposites were characterized using various apparatuses. In the nanocomposites, where the clay surface is pretreated with FA, FHA and CDFA, the basal spacing of the clay increased to 2.94, 3.26 and 3.80 nm, respectively The X-ray diffraction (XRD) and transmission electron microscopy (TEM) results confirmed the production of nanocomposites. PLA modified clay nanocomposites show higher thermal stability and significant improvement of mechanical properties in comparison with pure PLA.

Keywords: Nanocomposites, OMMTs, Poly(lactic acid)

Introduction

Petrochemical based polymer technology has given a lot of benefits to mankind. One of these benefits is the use of plastics in packaging. The most important factors determining rapid growth in the use of plastic in packaging industries are convenience, safety, low price and good aesthetic qualities. However the petrochemical-based polymers are produced from fossil fuel, consumed and discarded into environment, ending up as undegradable wastes. The increase of undegradable wastes are significantly disturbing and damaging to the environment. The environment specialists do not have the answer about how to deal with these undegradable wastes. Incineration of these wastes produces large amount of carbon dioxide that will contribute to global warming. Thus, there is a dire need for the development of green polymeric materials, which would not involve the use of toxic and noxious component in their manufacture and could be degradable in nature. For these reasons, through the world today, the development of biodegradable materials with the controlled properties has been a subject of great research challenge for the community of material scientists and engineers.

One of the most promising candidates for biodegradable synthetic polymers is PLA [1]. PLA can be obtained from renewable resources, therefore PLA represents a good candidate to produce disposable packaging in addition to its application in the textile industries, automotive and clinical uses [2-4]. Although PLA is an eco-friendly boiplastic with good biocompatibitity, poor hardiness, slow degradation, hydrophobicity, and lack of reactive side-chain groups limit its application [5]. Therefore, the modification of its properties to reach end-users demands is required.

*Corresponding author: emadaalmulla@yahoo.com

Various biodegradable and non-biodegradable plasticizers were used to improve processibility, and increase flexibility [6]. These aspects were carried out by modification some of the plasticizer properties: polarity, molecular weight, and end groups [7,8].

The incorporation of organoclays in the polymer to produce a nanocomposite was used to modify the property balance of a material. The improvements in thermal stability, physical and mechanical properties can be achieved by addition of 2-5 percent weight of organoclays in comparison to the neat polymer [9-11].

The modification of natural clay (montmorillonite) may carry out via exchanging the original inter-layer cations by organic cations where they are transformed from organophobic to organophilic materials and significantly increase the basal spacing of the clay layers [12]. It is generally accepted that the extent of swelling depends on the length of the alkyl chain and the cation exchange capacity of the clay [20]. Organoclays are mainly obtained by exchanging cations in the clay minerals, which contain hydrated Na^+ ions with alkylamidonium [21].

Preparation of PLA/thermoplastic starch/clay and PLA/ polycaprolactone/clay nanocomposites were investigated and characterized using X-ray diffraction, transmission electron microscopy and tensile measurements. The results show improvement in the tensile modulus and strength and a reduction in fracture toughness [22,23].

Plasticized PLA-based nanocomposites were prepared and characterized with epoxidized soybean oil and montmorillonite. It is reported that the organo-modified montmorillonite-based composites have shown the possible competition between the polymer matrix and the plasticizer for the intercalation between the alumino-silicate layers [5].

The present study shows preparation and characterization of new polymer nanocomposites using PLA and three

different FNCs synthesized from vegetable oil for modification of the montmorillonite. Organophilic montmorillonites were prepared by the cation exchange process.

Experimental

Materials

Sodium montmorillonite (Kunipia F) was obtained from Kunimine Ind. Co., Japan. Poly(lactic acid) and chloroform were purchased through local suppliers from T.J. Baker, USA and Merck, Germany, respectively.

Preparation of Organoclay

Organoclay was prepared with a cationic exchange process, where Na^+ in the montmorillonite was exchanged with alkylamidonium ion from FNCs synthesized from triacylglycerides, which were reported in our previous stydies [24-26], in an aqueous solution. 4.00 g of sodium montmorillonite (Na-MMT) was stirred vigorously in 600 m*l* of hot distilled water for one hour to form a clay suspension. Subsequently, a designated amount of FNCs, which had been dissolved in 400 m*l* of hot water and the desired amount of concentrated hydrochloric acid (HCl) was added into the clay suspension of FNCs. After being stirred vigorously for one hour at 80 °C, the organoclay suspension was filtered and washed with distilled water until no chloride was detected with a 1.0 M silver nitrate solution. It was then dried at 60 °C for 72 h. The dried organoclay was ground until the particle size was 75 μm before the preparation of the nanocomposite. The amounts of hydrochloric acid, and FNCs used in this study are listed in Table 1.

Table 1. The optimization of basal spacing of modified montmorillonite with different amounts of fatty nitrogen compounds and hydrochloric acid

Amount of FNCs (g) in 4.00 g of MMT	Conc. HCl (m*l*)	d-spacing (nm)		
		FA-MMT	FHA-MMT	CDFA-MMT
1.00	4.00	1.29	1.32	1.59
1.50	4.00	1.30	1.39	1.77
2.00	4.00	1.34	1.44	1.85
2.50	4.00	1.40	1.54	1.91
3.00	4.00	1.45	1.60	2.03
3.50	4.00	1.50	1.67	2.10
4.00	4.00	1.55	1.73	2.19
4.50	4.00	1.62	1.82	2.27
5.00	4.00	1.63	1.83	2.29
4.50	6.00	1.72	2.01	2.48
4.50	8.00	1.87	2.29	2.59
4.50	10.00	2.01	2.42	2.72
4.50	12.00	2.12	2.61	2.91
4.50	14.00	2.41	2.74	3.11
4.50	16.00	2.72	2.91	3.18
4.50	18.00	2.70	2.91	3.22

Preparation of PLA/Clay Nanocomposites

The required amount of PLA was dissolved in 50 m*l* of chloroform. The resultant mixture was stirred for 1 h. The required modified clay (FNCs-MMT) was then added into the dissolved PLA in the small portion. The mixture was then refluxed for 1 h and then ultrasonically stirred using the Ultra Sonic Cathode for 10 min to make sure that the clay was fully dispersed in the PLA solution. The nanocomposite was then poured into a Petri dish and left to dry. The amounts of PLA and modified clay used in this study are listed in Table 2.

Characterization

X-ray Diffraction (XRD) study was carried out using a Shimadzu XRD 6000 diffractometer with Cu-Kα radiation (λ=0.15406 nm). The diffractogram was scanned in the ranges from 2 to 10 ° at a scan rate of 1 °/min. The FTIR spectra of the samples were recorded by the FTIR spectrophotometer (Perkin Elmer FT-IR-Spectrum BX, USA) using the KBr disc technique. The thermal stability of the samples was studied by using the Perkin Elmer model TGA 7 Thermogravimetric Analyzer. The samples were heated from 35 to 800 °C with a heating rate of 10 °C/min under a nitrogen atmosphere with a nitrogen flow rate of 20 m*l*/min. The tensile strength, tensile modulus and elongation at break were measured by using the Instron Universal Testing Machine 4301 at 5 mm/min of crosshead speed in accordance to ASTMD638 [27]. Seven samples were used for the tensile test and the average of five results was taken as the resultant value. The dispersion of clay was studied by using Energy Filtering Transmission Electron Microscopy (EFTEM). TEM pictures were taken in a LEO 912 AB Energy Filtering Transmission Electron Microscope with an acceleration voltage of 120 KeV. The specimens were prepared using a Ultracut E (Reichert and Jung) cryomicrotome. Thin sections of about 100 nm were cut with a diamond knife at −120 °C.

Table 2. The amounts of PLA and modified clay in the nanocomposites

Sample identity	Weight of PLA (g)	Weight of EPO (g)	Weight of organoclay
mod0	4.00	1.00	0.00
mod1	3.96	0.99	0.05
mod2	3.92	0.98	0.10
mod3	3.88	0.97	0.15
mod4	3.84	0.96	0.20
mod5	3.80	0.95	0.25

mod0, mod1, mod2, mod3, mod4 and mod5= 0, 1, 2, 3, 4, and 5 % weight of organoclay, respectively.

Results and Discussion

The effect of clay content on the tensile properties of PLA/Na-MMT microcomposite, PLA/CDFA-MMT, PLA/FA-MMT, and PLA/FHA-MMT nanocomposites was shown in Figure 1. The reinforcing effect of unmodified montmorillonite in the PLA matrix was increased with a low increment rate. The maximum tensile strength was obtained when the clay content was 3 % of the weight. Further increase of the clay content decreases tensile strength. Ma-MMT acts as conventional particulate filler in the PLA matrix. Low tensile strength is obtained for PLA/Na-MMT because the clay-clay interactions are stronger than that of the PLA-clay interactions [28]. A poor compatibility between the clay and PLA matrix is expected as the mixing is at a micro level [29]. Figures 2 and 3 show a similar behavior of the clay content effect on the modulus and elongation at break of PLA/Na-MMT.

The increment of tensile strength, modulus, and elongation at break for the nanocomposites PLA with FA-MMT, FHA-MMT, and CDFA-MMT loadings are similar to that of the microcomposites. However, the rate of the increment of tensile properties for the nanocomposites increased.

Figures 1-3 show the highest tensile strength, modulus, and elongation at break of the PLA/FA-MMT, PLA/FHA-MMT, and PLA/CDFA-MMT nanocomposites were obtained when 5 % of the FA-MMT or the FHA-MMT and 3 % of the CDFA-MMT loadings are used. The enhancing effect of the FA-MMT, FHA-MMT, and CDFA-MMT on the mechanical properties is probably due to the increase of the amount of the incorporated PLA chains in the clay layers. The polymer-clay interactions include the interactions of the intercalated PLA chains with the surface layers of the silicates. However, the tensile strength modulus, and elongation at break decrease when the FA-MMT, FHA-MMT, and CDFA-MMT loadings are increased to more than 5 and 3 % of FA-MMT and FHA-MMT, and CDFA-MMT, respectively. The decrease of tensile strength, modulus, and elongation at break is due to the decrease of the PLA chains interacting with the clay as the clay coagglomerates. The tensile specimens were prepared as shown in Figure 4.

Bragg's law ($n\lambda=2d\sin\theta$) provides the condition for a plane wave to be diffracted by a family of lattice planes: d refers to the distance of two consecutive clay layers, where λ is the wavelength of the intercept X-rays at the incident angle θ. The presence of FNC chains in the galleries turns

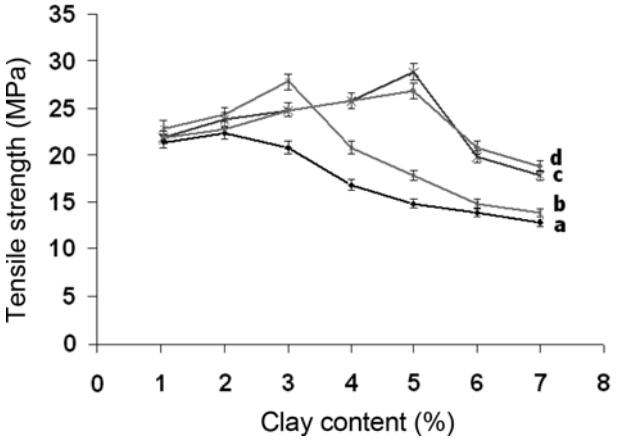

Figure 1. Effect of clay content on the tensile strength of (a) PLA/Na-MMT, (b) PLA/CDFA-MMT, (c) PLA/FA-MMT, and (d) PLA/FHA-MMT nanocomposites.

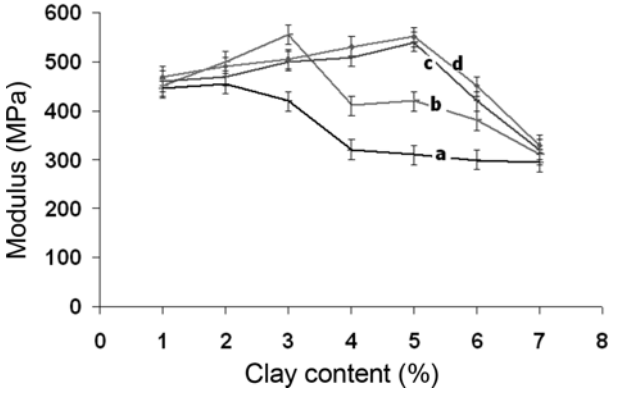

Figure 2. Tensile modulus of (a) PLA/FA-MMT, (b) PLA/CDFA-MMT, (c) PLA/FA-MMT, and (d) PLA/FHA-MMT nanocomposites.

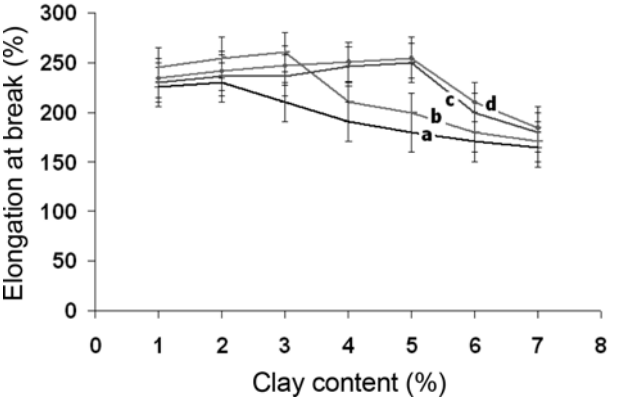

Figure 3. Elongation at break of (a) PLA/FA-MMT, (b) PLA/CDFA-MMT, and (c) PLA/FHA-MMT nanocomposites.

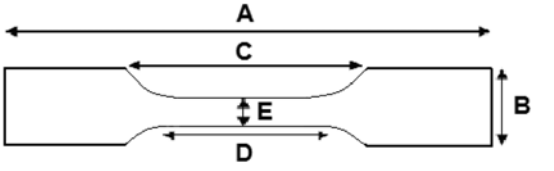

Figure 4. Dumbbell dimension diagram for tensile test; (A) length of test specimen (75 mm), (B) width of test specimen (12.5 mm), (C) length (25 mm), (D) length of bench marker (20 mm), and (E) width (4 mm).

the original hydrophilic silicate to an organophilic silicate, and thus increases the layer-to-layer spacing of Na-MMT [17]. By using X-ray diffraction, Na-MMT shows a d001 diffraction peak at 2θ=7.21 °, which assigns the interlayer distance of the natural montmorillonite with a basal spacing of 1.23 nm. Na-MMT was surface treated with FNC as an intercalation agent through a cation exchange process. The cationic head groups of the intercalation agent molecule would preferentially reside at the surface layer and the aliphatic tail will radiate a ways from the surface.

Table 1 shows the optimum amount of FNCs and HCl to reach maximum d-spacing were studied. It was found that the maximum d-spacing was achieved when the amount of FNC and HCl were 4.50 g and 16 m*l*, respectively. It was observed that there was no significant increase in d-spacing with a further increase in FNCs and HCl. The maximum basal spacing of FA-MMT, FHA-MMT, and CDFA-MMT increases from 1.23 to 2.69, 2.89 and 3.21 nm, respectively (Table 3), indicating that these FNCs were successfully intercalated into the Na-MMT galleries.

Greater basal spacing is observed for the CDFA-MMT than that of the FHA-MMT and FA-MMT, suggesting that CDFA adopts a paraffin arrangement in the silicate layer while a monolayer arrangement of FHA and FA molecules is formed in the interlayer spacing of Na-MMT [30].

Table 4 shows the XRD patterns of the nanocomposites prepared using three different FNC (alkylamidonium groups) modified montmorillonite nanocomposites. In the nanocomposites where the montmorillonite surface is pretreated with FA and FHA, the basal spacing of the clay increased to 2.94 and 3.26 nm, respectively. However, when the montmorillonite surface is pretreated with CDFA, which has two fatty acid chains, the basal spacing further increases to 3.80 nm. This clearly shows that the basal spacing of organoclay in the polymer matrix increases with the increase in the size of the surfactant as was observed by Agag and Takeichi [31]. These XRD patterns also suggest that all the nanocomposites produced are intercalated compounds.

Table 3. Diffraction angle and basal spacing of natural clay (Na-MMT) and modified clays with the FA-MMT, FHA-MMT and CDFA-MMT

Sample	Exchanged cation	2 Theta (degree)	d-spacing (nm)
Na-MMT	Na^+	7.21	1.23
FA-MMT	$RCO\text{-}N^+H_3$	3.29	2.67
FAH-MMT	$RCO\text{-}N^+H_2OH$	3.06	2.88
CDFA-MMT	$(RCO)_2\ NHCON^+H_2$	2.76	3.19

Table 4. Diffraction angle and basal spacing of PLA/FNCs modified clay nanocomposites

Sample	2 Theta (degree)	d-spacing (nm)
PLA/MMT	6.91	1.27
PLA/FA-MMT	3.00	2.94
PLA/FHA-MMT	2.70	3.26
PLA/CDFA-MMT	2.16	3.80

The FTIR spectra of Na-MMT show peaks at 3510, 1625 and 1010 cm^{-1} are due to the O-H stretching, interlayer water deformation and the Si-O stretching vibration, respectively. The other strong band absorption at 512 and 440 cm^{-1} indicate the presence of Al-O stretching and Si-O bending, respectively in the clay. The FTIR spectra of the FA MMT, FHA-MMT, and CDFA-MMT show the major bands of FA, FHA, and CDFA spectra [24-26] in addition to the bands of the original Na-MMT. The band at around 1470 cm^{-1} suggests the existence of the ammonium ion. Therefore, these indicate that the FA, FHA, and CDFA were intercalated in the silicate layers. Figure 5 shows the FTIR spectra of Na-MMT, FA-MMT, FHA-MMT, and CDFA-MMT.

Most of the thermoanalytical studies reveal new insights into the structure of intercalated clays [32]. Thermogravimetric analysis (TGA) gives information on the structure of the intercalating molecules by the weight loss steps. Thermal degradation of MMT shows two steps [33]. The first one is before 200 °C because of the volatilization of water adsorbed on the external surfaces of the MMT and water inside the

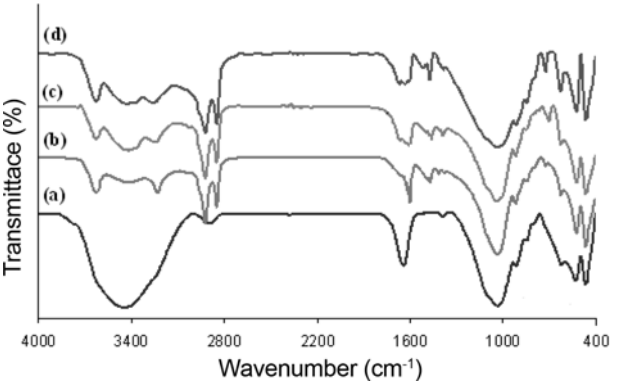

Figure 5. FTIR spectra of (a) Na-MMT, (b) FA-MMT, (c) FHA-MMT, and (d) CDFA-MMT.

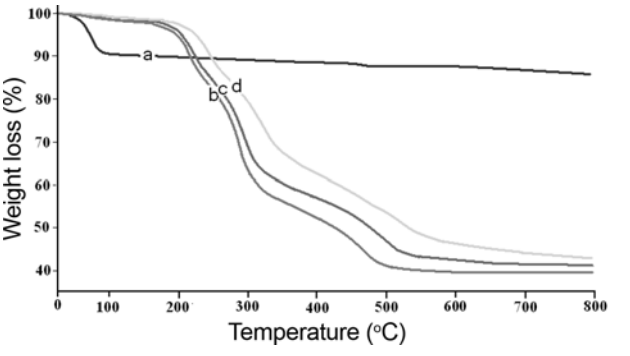

Figure 6. TGA thermograms of (a) MMT, (b) FA-MMT, (c) FHA-MMT, and (d) CDFA-MMT.

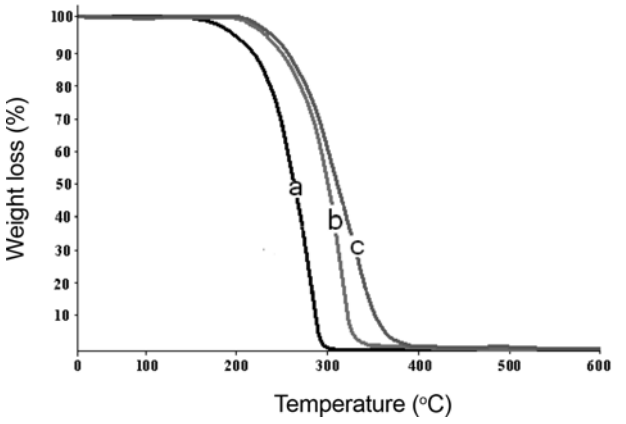

Figure 7. TGA thermograms of (a) FA, (b) FHA, and (c) CDFA.

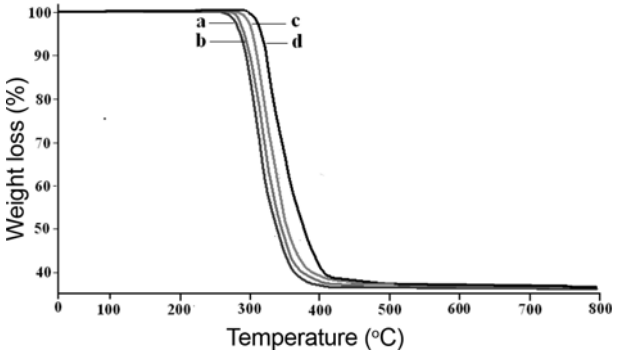

Figure 8. TGA thermograms of (a) pure PLA, (b) PLA/FA-MMT, (c) PLA/FHA-MMT, and (d) PLA/CDFA-MMT nanocomposites.

interlayer space. The second step is in the range from 500 to 1000 °C due to the loss of hydroxyl groups of the MMT structure. The thermal degradation of the modified MMT can be explained in four steps. The first step occurs at below 200 °C due to the vaporization of water. Decomposition of the surfactant takes place in the second step between 200-500 °C. Dehydroxylation of the aluminosilicates at the temperature range of 500-800 °C happens in the third step. In the last step, the organic carbon reacts with inorganic oxygen (combustion reaction) at about 800 °C.

The weight loss curves (TGA) of the MMT, FA-MMT, FHA-MMT, and CDFAMMT were illustrated in Figure 6. MMT contains water due to hydrated sodium (Na^+) cations intercalated inside the clay layers. The presence of alkyl-amidonium groups within the MMT interlayer spacing lowers the surface energy of the inorganic structure and will transform organophobic to organophilic materials. The major difference between the thermogram of the unmodified clay and that of the organoclay is that the organic constituents in the organoclay decompose in the range from 200 to 500 °C, as the organic constituent in the organoclay decomposes in this range. Figure 7 shows that the FA decomposed as the temperature increased from 155 to 600 °C. The decomposition process ended at 312 °C. The FHA started decomposing at higher temperatures than that of the FA, which started at 190 °C and ended at 355 °C. CDFA had the highest decomposition temperature (starting at 197 °C and ending at 396 °C). It can be observed that the decomposition temperatures of the FA-MMT, FHA-MMT and CDFA-MMT were higher

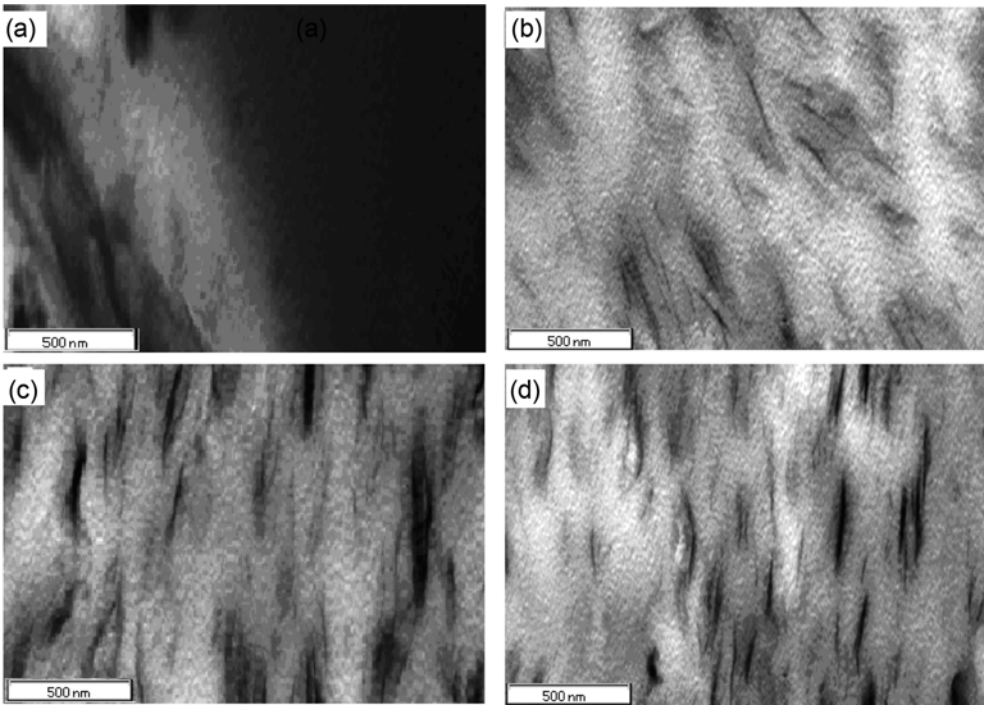

Figure 9. TEM micrographs of (a) PLA Na-MMT, (b) PLA/CDFA- MMT, (c) PLA/FA-MMT, and (d) PLA/FHA-MMT composites.

than those of the pure FA, FHA, and CDFA. The increase in the decomposition temperatures of these FNCs in the organoclays implies that there is a strong intermolecular interaction between the alkylamidonium cations and the clay. In other words, after the ion exchange the FNC is intercalated and attached to the silicate layers of the clay and hence their decomposition temperatures increase.

Thermogravimetric analyses were done on PLA/FNCs-MMT nanocomposites in order to determine the effect of modified clay content in the polymer matrix on thermal properties. The results of TGA are shown in Figure 8. The onset of the degradation of the nanocomposites (Figure 8) is higher, that is 282, 285, and 294 °C, for PLA containing FA-MMT, FHA-MMT, and CDFA-MMT, respectively, compared to the PLA blend (268 °C). The results show that the thermal stability increases with addition of the FNCs. The presence of silicate layers dispersed homogeneously in the polymer sheet hinders the permeability of volatile degradation products out from the material and helps delay the degradation of the nanocomposites [34].

Transmission electron microscopy (TEM) micrographs of the PLA composites reinforced with Na-MMT, CDFA MMT, FHA-MMT, and FA-MMT were shows in Figures 8(a), (b), (c), and (d), It can be seen in Figure 8(a) that the original Na-MMT stack morphology was fully preserved with PLA due to the incompatible nature of both constituents. The dark lines represent the thickness of the individual clay layers or agglomerates. In Figures 8(c) and 8(d), the organoclay does not show its original layered structure and it is quite dispersed in the PLA matrix, especially in the presence of the PLA/FA-MMT and PLA/FHA-MMT. The related structure can be referred to as intercalated lamellae, tactoids composed of a variable number of lamellae and aggregates of tactoids. A higher degree of intercalation and some exfoliated zones was observed in the TEM micrograph of PLA/CDFA-MMT (Figure 8(b)). This is maybe due to the effect of two long chains of fatty acids in CDFA.

Conclusion

New polymer nanocomposites were prepared using PLA and clay modified by FNCs. Organophilic montmorillonites (FA-MMT, FHA-MMT, and CDFA-MMT) were successfully prepared by the cation exchange process. FTIR spectra indicate the presence of an alkylamidonium group resulting from the modification. Thermogravimetric analysis shows that the decomposition temperature of FA, FHA, and CDFA in the organoclay is higher compared with that of the pure FNCs, suggesting that there is a strong intermolecular interaction between the alkylamidonium and the montmorillonite. PLA clay nanocomposites have been prepared by incorporating 5 % CDFA-MMT and 3 % of both FA-MMT and FHA-MMT. TEM analysis shows that the prepared nanocomposites were of the intercalated (FA-MMT and FHA-MMT) and partially exfoliated types (CDFA-MMT). The TGA thermograms of PLA/clay nanocomposites have higher decomposition temperatures in comparison with that of PLA composites. The XRD patterns revealed that the interlayer distance of organoclays in the PLA blend were significantly increased. The use of FNCs for clay modification will reduce the dependence on petroleum-based surfactants. In addition to biodegradable, these nanocomposites are considerable as renewable resources, environmentally friendly.

References

1. Y. Lemmouchi, Murariu M, A. Santos, A. Schacht, and P. Dubois, *Eur. Polym. J.*, **45**, 2839 (2009).
2. H. Tsuji and Y. Ikada, *J. Appl. Polym. Sci.*, **67**, 405 (1998).
3. T. Iwata and Y. Doi, *Macromolecules*, **31**, 2461 (1998).
4. D. Sawai, K. Takahashi, T. Imamura, K. Nakamura, T. Kanamoto, and S. Hyon, *Polym. Sci. Polym. Phys.*, **40**, 95 (2002).
5. E. Al-mulla, A. Suhail, and S. Aowda, *Ind. Crops Prod.*, **33**, 23 (2011).
6. R. Auras, S. Singh, and J. Singh, *Packag Technol. Sci.*, **18**, 207 (2005).
7. R. Auras, B. Harte, S. Selke, and R. Hernandez, *J. Plastic. Film. Sheet.*, **19**, 123 (2003).
8. A. Nijenhuis, E. Colstee, and D. Grijpma, *Pennings, Polymer*, **37**, 5849 (1996).
9. L. Liu, S. Li, H. Garreau, and M. Vert, *Biomacromol*, **1**, 350 (2000).
10. N. Lopez-Rodriguez, A. Lopez-Arraiza, E. Meaurio, and J. Sarasua, *Polym. Eng. Sci.*, **46**, 1299 (2006).
11. Y. Li and H. Shimizu, *Macromol. Biosci.*, **7**, 921 (2007).
12. M. Baiardo, G. Frisoni, M. Scandola, M. Rimelen, D. Lips, K. Ruffieux, and E. Wintermantel, *J. Appl. Polym. Sci.*, **90**, 1731 (2003).
13. N. Ogata, H. Sasayama, K. Nakane, and T. Ogihara, *J. Appl. Polym. Sci.*, **89**, 474 (2003).
14. Z. Kulinski and E. Piorkowska, *Polymer,* **46**, 10290 (2005).
15. Z. Ren, L. Dong, and Y. Yang, *J. Appl. Polym. Sci.*, **101**, 1583 (2006).
16. P. LeBaron, Z. Wang, and T. Pinnavaia, *Appl. Clay. Sci.*, **15**, 11 (1999).
17. M. Alexandre and P. Dubois, *Mater. Sci. Eng. R. Rep.*, **28**, 1 (2000).
18. A. Okada and A. Usuki, *Macromol. Mater. Eng.*, **291**, 1449 (2006).
19. E. Giannelis, *Adv. Mater.,* **8**, 29 (1996).
20. B. Zidelkheir1 and M. Abdelgoad, *J. Therm. Anal. Cal.*, **94**, 181 (2008).
21. A. Pérez-Santano, R. Trujillano, C. Belver, A. Gil, and M. Vicente, *J. Colloid. Interface. Sci.*, **284**, 239 (2005).
22. O. Arroyo, M. Huneault, B. Favis, and M. Bureau, *Polym. Compos.*, **31**, 114 (2010).

23. W. Hoidy, E. Al-Mulla, and K. Al-Janabi, *J. Polym. Environ*., **18**, 608 (2010).
24. E. Al-Mulla, W. Yunus, N. Ibrahim, and M. Rahman, *J. Oleo Sci*., **58**, 467 (2009).
25. W. Hoidy, M. Ahmad, E. Al-Mulla, W. Yunus, and N. Ibrahim, *J. Oleo Sci*., **59**, 15 (2010).
26. E. Al-Mulla, W. Yunus, N. Ibrahim, and M. Rahman, *J. Oleo Sci.,* **59**, 80 (2010).
27. ASTM D638-03, Standard Test Method for Tensile Properties of Plastics, 2004.
28. Y. Vu, J. Mark, L. Pham, and M. Engelhardt, *J. Appl. Polym. Sci*., **82**, 1391 (2001).
39. M. Arroyo, M. Lopez-Manchado, and B. Herrero, *Polymer*, **44**, 2447 (2003).
30. M. Pospisil, A. Kalcndova, P. Capkova, J. Simonik, and M. Valaskova, *J. Colloid. Interface Sci.,* **227**, 154 (2004).
31. T. Agag and T. Takeichi, *Polymer,* **41**, 7083 (2000).
32. Y. Xi, W. Martens, H. He, and R. Frost, *J. Therm. Anal. Cal*., **81**, 91 (2005).
33. M. Manchado and B. Herrero, *Polymer,* **44**, 2447 (2003).
34. S. Jamaliah, M. Wan, Z. Khairul, M. Dahlan, and A. Mansor, *Polym. Test*, **24**, 211 (2005).